Clinical & Experimental Immunology
The Journal of Translational Immunology

Clinical and Experimental Immunology ORIGINAL ARTICLE doi:10.1111/cei.12635

Increased lymphocyte apoptosis in mouse models of colitis upon ABT-737 treatment is dependent upon BIM expression

C. Lutz,*[1] M. Mozaffari,*[1] V. Tosevski,[†] M. Caj,* P. Cippà,[‡] B. L. McRae,[§] C. L. Graff,[§] G. Rogler,* M. Fried* and M. Hausmann*

*Division of Gastroenterology and Hepatology, Department of Internal Medicine, University Hospital Zurich, [†]Flow Cytometry Facility, University Zürich, [‡]Division of Nephrology, University Hospital Zurich, Switzerland, and [§]AbbVie Bioresearch Center, AbbVie Worcester, MA, USA

Accepted for publication 10 March 2015
Correspondence: M. Hausmann, Clinic of Gastroenterology and Hepatology, Department of Internal Medicine, LAB H14, University Hospital of Zürich, CH-8091 Zürich.
E-mail: martin.hausmann@usz.ch

[1]These authors contributed equally to this study.

Summary

Exaggerated activation of lymphocytes contributes to the pathogenesis of inflammatory bowel disease (IBD). Medical therapies are linked to the BCL-2 family-mediated apoptosis. Imbalance in BCL-2 family proteins may cause failure in therapeutic responses. We investigated the role of BCL-2 inhibitor ABT-737 for lymphocyte apoptosis in mice under inflammatory conditions. B.6129P2-interleukin (IL)-10^{tm1Cgn}/J (*IL-10*$^{-/-}$) weighing 25–30 g with ongoing colitis were used. Fifty mg/kg/day ABT-737 was injected intraperitoneally (i.p.). Haematological analyses were performed with an ADVIA 2120 flow cytometer and mass cytometry with a CyTOF 2. Following i.p. administration, ABT-737 was detected in both spontaneous and acute colitis in peripheral blood (PBL) and colon tissue. Treatment led to lymphopenia. CD4$^+$CD44$^+$CD62L$^+$ central memory and CD8$^+$, CD44$^+$ CD62L$^-$ central memory T cells were decreased in PBL upon ABT-737 compared to vehicle-receiving controls. Increased apoptosis upon ABT-737 was determined in blood lymphocytes, splenocytes and Peyer's patches and was accompanied by a decrease in *TNF* and *IL-1B*. ABT-737 positively altered the colonic mucosa and ameliorated inflammation, as shown by colonoscopy, histology and colon length. A decreased *BIM*/*BCL-2* ratio or absence of BIM in both *Bim*$^{-/-}$ and *Il10*$^{-/-}$ × *Bim*$^{-/-}$ impeded the protective effect of ABT-737. The *BIM*/*BCL-2* ratio decreased with age and during the course of treatment. Thus, long-term treatment resulted in adapted *TNF* levels and macroscopic mucosal damage. ABT-737 was efficacious in diminishing lymphocytes and ameliorating colitis in a BIM-dependent manner. Regulation of inappropriate survival of lymphocytes by ABT-737 may provide a therapeutic strategy in IBD.

Keywords: ABT-737, apoptosis, BCL-2, BIM, IBD, mucosal T cell turnover

Introduction

The BCL-2 family plays a critical role in controlling immune responses by regulating the expansion and contraction of the activated lymphocyte population via apoptosis. The majority of activated T cells die at the end of a T cell response, which coincides with the exhibition of decreased levels of BCL-2 just before they begin to die *in vivo* [1]. A decrease of the prosurvival BCL-2 contributes to apoptosis of activated T cells [2]. In patients suffering from inflammatory bowel disease (IBD), the lifespan of antigen-primed and activated T cells is extended and an abnormal population of activated T cells is retained within the mucosal compartment [3–5]. Enhanced expression of anti-apoptotic BCL-2 is found in lamina propria lymphocytes from inflamed Crohn's disease (CD) tissue after CD2 pathway stimulation [3]. An elevated BCL-2 level is also found in cultures of unstimulated T cells isolated from inflamed CD tissue [3]. Lamina propria T cells in CD show activation of the signal transducer and activator of transcription 3 (STAT-3) signalling pathway in response to interleukin (IL)-6. STAT-3 mediates the expression of anti-apoptotic genes such as *BCL*-2 and *BCL*-XL [6]. Resistance of CD T cells to apoptotic signals is correlated with an increased BCL-2 expression [3]. This is supported further by reports of a higher BCL-2/BAX

ratio in CD mucosa compared to controls [4] as well as a resistance to Fas-induced apoptosis in peripheral T cells acquired from CD patients [7]. Apoptosis of anti-inflammatory regulatory T cells (T_{reg} cells) is reduced in both mucosal and peripheral $CD4^+CD25^{high}$forkhead box protein 3 $(FoxP3)^+$ T_{reg} cells of IBD patients [8].

Anti-apoptotic BCL-2 interacts with the pro-apoptotic BH3-only protein family member BIM to regulate the survival of lymphocytes. The summary effect of the interaction between BCL-2 and BIM is dependent upon the cell type, but is also tissue-specific, whereby BCL-2 promotes the survival of naive T cells [9]. Indeed, naive T cells from $Bim^{+/-}$ $Bcl\text{-}2^{-/-}$ mice die at an accelerated rate *in vitro*. BCL-2 is critical in preventing the pro-apoptotic effects of BIM in naive $CD8^+$ T cells *in vivo*, but molecules other than BCL-2 may antagonize BIM in $CD4^+$ cells. BIM controls T cell numbers in the periphery by promoting apoptosis and/or decreasing their thymic production. *Bim*-deficient mice have elevated numbers of normal single-positive T cells in the periphery [10]. Furthermore, BIM is a primary trigger for killing B cells during their development [11]. *Bim* deficiency prevents the death of activated T cells *in vitro* and *in vivo*, suggesting that the protective effect of BCL-2 is mediated solely by neutralization of BIM [2].

IBD affects about one in 150 people in the industrialized world. IBD is characterized by a chronic inflammation of the intestinal wall and comprises two main conditions, namely ulcerative colitis (UC) and CD. In the pathogenesis of IBD this inflammatory state is sustained by an exaggerated response of T lymphocytes to luminal antigens associated with an increased resistance to the induction of apoptosis [4].

The central elements of medical therapy consist of sulphasalazine, aminosalicylates, steroids, immunomodulators and biologicals [12,13]. Medical therapies that regulate lymphocyte proliferation and contraction are linked directly to the BCL-2 family-mediated apoptosis. Sulphasalazine is a potent pro-apoptotic agent [14], as confirmed in peripheral blood lymphocytes from CD patients and in lamina propria T lymphocytes isolated from inflammatory lesions in CD patients. Induction of apoptosis by sulphasalazine is associated with a decrease in anti-apoptotic BCL-XL and BCL-2. Glucocorticoids inhibit the synthesis of IL-1 and IL-2, resulting in the suppression of the T cell-dependent immune reaction and T cell proliferation [15]. Azathioprine (AZA) is an immunosuppressive agent which interferes with T cell proliferation via its metabolite 6-thioguanin-nucleotide. AZA therapy reduces natural killer cells in blood and lamina propria by increasing apoptosis [16]. Increased early and late apoptosis upon AZA was determined in $CD4^+$ T cells from peripheral blood isolated from control patients but not from CD patients [17]. BCL-XL is suppressed by AZA, therefore leading to apoptosis through a mitochondrial pathway [18]. Anti-tumour necrosis factor (TNF) antibodies are used in CD and UC to induce and maintain remission. Infliximab was shown to induce apoptosis and an increase in the Bax/Bcl-2 ratio of CD3/CD28 stimulated Jurkat T cells [19]. Furthermore, the activation of BAX and BAK triggers apoptosis in lamina propria lymphocytes and monocytes by activating the caspase family and inducing cytochrome c release [20]. Administration of all clinically effective anti-TNF antibodies resulted in a significant induction of T cell apoptosis in IBD when lamina propria $CD4^+$ T cells expressing TNF-$R2^+$ were co-cultured with $mTNF^+CD14^+$ intestinal macrophages [21].

Boosting the initiation of cell death in apoptosis-resistant lymphocytes could improve the success of medical therapy. ABT-737 (AbbVie; AbbVie Bioresearch (Chicago, IL, USA) is a potent inhibitor of BCL-2, BCL-XL and BCL-W [22,23] and has been shown to disrupt the interactions of BCL-2 family proteins to induce apoptosis in cancer. ABT-737 inhibits BCL-2 by directly blocking BIM-binding sites and displacing BIM, which becomes freely available to interact with other BCL-2 molecules in the cell. Additionally, BIM can bind to BAX and BAK to trigger apoptosis by initiating the formation of pores on the mitochondrial surface. ABT-737 is a BH3-only mimetic that shows a potent action against various transformed cells while exhibiting minimal toxicity towards normal cells. ABT-737 is effective in treating animal models of autoimmune diseases [24], arthritis [25] and lupus [26]. Furthermore, expression of BIM, and the extent of its association with BCL-2, correlates with *in vivo* ABT-737 sensitivity [27].

Our own studies on apoptosis of lymphocytes in the intestinal mucosa revealed that cell death in Peyer's patches is dependent on the pro-apoptotic protein BIM [28]. Based on these findings, we investigated the role of ABT-737 in the cell death of lymphocytes in mice under inflammatory conditions.

Materials and methods

Ethical considerations

The experimental protocol was approved by the local Animal Care Committee of the University of Zurich (Cantonal Ethics Committee of Zurich, 162/2011).

ABT-737 treatment

ABT-737 was provided by AbbVie Bioresearch and was injected intraperitoneally (i.p.) at a dose of 50 mg/kg/day. The vehicle consisted of polyethylene glycol, Tween 80, dextrose solution and dimethylsulphoxide (DMSO).

Murine colitis models

Acute dextran sulphate sodium (DSS)-induced colitis. B6.129-Bcl2l11tm1.1Ast/J ($Bim^{-/-}$) mice were kindly provided by Professor Dr Andreas Villunger (Division for

Developmental Immunology, Innsbruck Medical University). *Bim*$^{-/-}$ mice were back-crossed for at least 12 generations. Acute colitis was induced in female C57-BL/6J-Fue and *Bim*$^{-/-}$ mice by administration of 2% DSS for 9 days. Mice weighing 20–25 g were used for the experiments and housed in individually ventilated cages (IVC). All animals were housed for at least 3 weeks prior to testing in a specific pathogen-free (SPF) facility. Animals were killed on day 9. Acute DSS-induced colitis is an animal model for acute intestinal barrier disturbance and acute damage.

Spontaneous colitis.
B.6129P2-Il10^{tm1Cgn}/J (*Il10*$^{-/-}$, mice were ordered from The Jackson Laboratory, Bar Harbor, ME, USA, and were already back-crossed to the C57BL/6J genetic background for several generations) and B.6129P2-IL-10^{tm1Cgn}/J × B6.129-Bcl2l11$^{tm1.1Ast}$/J (*Il10*$^{-/-}$ × *Bim*$^{-/-}$) develop colitis after 12–15 weeks under SPF conditions. *Il10*$^{-/-}$ weighing 25–30 g were used for the experiments. Animals were killed on day 14 of ABT-737 treatment. The IL-10$^{-/-}$ model of colitis reflects the exaggerated immune reaction against the endogenous gut flora as seen in CD patients. *Il10*$^{-/-}$ have a low penetrance of disease when raised under SPF conditions, and therapeutic studies in this model are difficult to perform. Therefore we defined a clearly visible rectal prolapse as an external visible indicator of ongoing colitis in our *Il10*$^{-/-}$ colony, as also stated in the Results section, whenever *Il10*$^{-/-}$ suffering from ongoing colitis were used.

Assessment of colonoscopy and histological score in mice

Animals were anesthaetized with isoflurane and examined with the Tele Pack Pal 20043020 (Karl Storz Endoskope, Tuttlingen, Germany) and scored according to the murine endoscopic index of colitis severity (MEICS), as described previously [29]. For assessment of the histological scores, 1 cm of the distal third of the colon was removed and scored as described [30,31].

Cell isolation

Murine peripheral blood lymphocytes were used for mass cytometric analyses. Whole blood was collected in ethylenediamine tetraacetic acid (EDTA)-treated collection tubes (BD vacutainer, ref. 367525; BD Biosciences, San Jose, CA, USA). ACK (1·5 M NH_4Cl, 100 mM $KHCO_3$, 10 mM Triplex111, pH 7·2) lysing buffer was used for lysing red blood cells.

Splenocytes were isolated using the gentle magnetic affinity cell sorting (gentleMACS) octo dissociator (Miltenyi Biotec, San Diego, CA, USA; no. 130-095-937) and gentleMACS C tubes (Miltenyi Biotec; no. 130-093-237). One mouse spleen was transferred into a gentleMACS C tube containing 10 ml ACK. A single-cell suspension was obtained by using the gentleMACS octo dissociator program m_spleen 03 three times. Splenocytes were passed over a 70-μm mesh filter and centrifuged. Cells were resuspended in 1 ml ACK, centrifuged, resuspended in phosphate-buffered saline (PBS) and passed again over a 70-μm mesh filter to obtain 200–300 × 10^6 splenocytes/spleen.

Lamina propria mononuclear cells (LPMNC) from small bowel were isolated with the help of the lamina propria dissociation kit (Miltenyi Biotec; no. 130-097-410), according to the manufacturer's protocol.

Mass cytometry, staining, data acquisition and analysis

Single-cell suspensions obtained from peripheral blood, spleen and lamina propria were stained according to the manufacturer's recommendations (MaxPar Cell Surface Staining Protocol and MaxPar Cytoplasmic/Secreted Antigen Staining Protocol; DVS Sciences, Toronto, Canda). In short, for viability staining cells were washed with PBS and resuspended in PBS to a maximum concentration of 1 × 10^7/ml. Cell-ID cisplatin reagent (Fluidigm, San Francisco, CA, USA; cat. no. 201064) was added to a final concentration of 5 μM. Following 5 min incubation at room temperature, samples were washed with cell staining buffer (Fluidigm; cat. no. 201068) by adding 5× the volume of the initial cell suspension. Each sample was resuspended in a volume of 50 μl cell staining buffer and 50 μl of the surface antibody cocktail was added (MaxPar Mouse Spleen/Lymph Node Phenotyping Panel Kit, cat. no. 201306). Following 30 min incubation at room temperature, samples were washed twice with 2 ml of cell staining buffer each and fixed by adding 1 ml of 1× MaxPar Fix I Buffer (Fluidigm; cat. no. 201065) to each tube, gently vortexed and incubated at room temperature for an additional 15 min. Cells were washed twice with 2 ml MaxPar Perm-S buffer each (Fluidigm; cat. no. 201066) and resuspended in 50 μl of the same buffer. The intracellular antibody cocktail (MaxPar Mouse Intracellular Cytokine I Panel Kit, cat. no. 201310) was added to each sample in 50 μl volume and incubated for 30 min at room temperature. Following two washing steps with 2 ml of cell staining buffer each, cells were labelled with 1 ml of 100 nM iridium intercalation solution (Fluidigm; cat. no. 201192B) in MaxPar Fix and Perm buffer (Fluidigm; cat. no. 201067) at 4 °C overnight. Cells were washed twice with 2 ml cell staining buffer each and once with water (Ultrapure Mili-Q water, 18·2 MΩ*cm at 25°C; Merck Milipore, Darmstadt, Germany). Cells were left pelleted until ready for acquisition, at which point their concentration was adjusted to 1–1·5 × 10^6 cells/ml in the Ultrapure Mili-Q water.

Cells were acquired on the CyTOF 2 instrument (Fluidigm) with an acquisition flow rate of 0·045 ml/min and

following data processing settings (default thresholding scheme, lower convolution threshold of 200 IU, minimum event duration of 12 pushes, maximum event duration of 100 pushes, noise reduction active). All samples were spiked with EQ four-element calibration beads during acquisition (Fluidigm; cat. no. 201078) and resulting FCS files were normalized according to the built-in normalization algorithm (CyTOF software version 6·0·626) to account for intra- and intersample intensity measurement variability. The resulting data were analysed with FlowJo (Flowjo LLC; TreeStar, Inc., Ashland, OR, USA) and Cytobank (Cytobank Inc., Mountain View, CA, USA) software.

Blood analyses

Haematological analyses were performed by the Division of Hematology at the University Hospital Zurich with an ADVIA 2120 flow cytometer (Siemens, Eschborn, Germany).

RNA extraction and quantitative real-time polymerase chain reaction (PCR)

Total RNA was extracted using the RNeasy Mini Kit (Qiagen, Basel, Switzerland). mRNA was reverse-transcribed into cDNA using the high-capacity cDNA reverse transcription kit (Applied Biosystems, Waltham, MA, USA). *Bim* (no. Mm00437796_m1; Applied Biosystems), *Bcl-2* (no. Mm00477631_m1*), *TNF* (no. Mm99999068_m1) and *IL1b* (no. Mm01336189_m1) gene expression was determined with a *Taq*Man® gene expression assay. Actin gene expression was measured as endogenous control (no. 4352341E; Applied Biosystems) and used for the calculation of relative mRNA expression using the ΔΔCt method. All samples were analysed as triplicates.

Analysis of apoptosis and flow cytometry

Apoptosis was quantified by terminal deoxynucleotidyl transferase dUTP nick end labelling (TUNEL) technology with the In Situ Cell Death Detection Kit (no. 11684795910; Roche, Mannheim, Germany), as described by the manufacturer.

Numbers of living and apoptotic cells were determined by flow cytometry of annexin V- and propidium iodide (PI)-stained cells. Cells were resuspended in annexin V binding buffer, as indicated by the manufacturer, and stained with allophycocyanin (APC)-conjugated annexin V (Enzo Life Science, Basel, Switzerland; diluted 1 : 40) and PI (Sigma-Aldrich, St Louis, MO, USA; final concentration 25 μg/ml). Annexin V^-/PI^- cells were considered alive; apoptotic cells displayed staining for annexin V but not for PI.

Fluorescence was measured by flow cytometry using a BD fluorescence activated cell sorter (FACS)Canto II flow cytometer equipped with two lasers (excitation wave lengths: 488 and 633 nm). CD4 was stained with anti-mouse antibody from ImmunoTools (no. 22150043sp, 1 : 1000). CD8 was stained with anti-mouse antibody from ImmunoTools (Friesoythe, Germany; no. 22150083sp, 1 : 1000). Both primary antibodies were directly conjugated with fluorescein isothiocyanate (FITC).

Statistical analyses

Real-time PCR data were calculated from triplicates. Statistical analyses were performed using PASW statistics version 18·0 (SPSS Inc., Chicago, IL, USA). Kruskal–Wallis non-parametric analysis of variance and Bonferroni-corrected Mann–Whitney rank-sum tests were applied for animal experiments. Box-plots express median with relative quartiles, minimum and maximum. One-way analysis of variance (ANOVA) and Tukey's *post-hoc* test were used for cell culture experiments. Bars represent mean values with whiskers displaying standard deviation. Differences were considered significant at $P < 0{\cdot}05$ (*), highly significant at $P < 0{\cdot}01$ (**) and very highly significant at $P < 0{\cdot}001$ (***).

Results

ABT-737 is detected in blood and intestine following i.p. administration

ABT-737 was applied in the $Il10^{-/-}$ model of spontaneous colitis. A calculated dose of 50 mg/kg/day was injected i.p. for 14 days. Control mice received a corresponding dose of vehicle solution during the same time-period. No treatment-related death or evidence of infection was observed in any of the animals. Water consumption was not reduced in mice treated with ABT-737 compared to controls. Peripheral blood, faeces, intestinal epithelial cells (IEC) and whole colon tissue of mice were harvested ($n = 4$ each). Using mass spectrometric (MS) quantification, ABT-737 could be detected in the peripheral blood. Following 14 days of treatment, ABT-737 was localized in peripheral blood ($0{\cdot}47 \pm 0{\cdot}26$ μg/μl), faeces ($9{\cdot}44 \pm 4{\cdot}12$ μg/g), IECs ($6{\cdot}07 \pm 6{\cdot}20$ μg/g) and whole colon tissue ($3{\cdot}67 \pm 3{\cdot}91$ μg/g). This confirms that following i.p. administration ABT-737 indeed reaches the peripheral blood. MS quantification proved the presence of ABT-737 in whole colon tissue, its uptake into IEC and its accumulation in the faeces.

Additionally, ABT-737 was applied in the murine model of acute DSS-induced colitis; 50 mg/kg/day was injected i.p. for 9 days. By MS quantification, ABT-737 could be detected in the peripheral blood ($0{\cdot}74 \pm 0{\cdot}37$ μg/μl), faeces ($29{\cdot}96 \pm 21{\cdot}17$ μg/g), IECs ($1{\cdot}61 \pm 2{\cdot}90$ μg/g) and whole colon tissue ($7{\cdot}17 \pm 0{\cdot}93$ μg/g).

ABT-737 induces a significant lymphopenia in mouse models of colitis

Flow cytometry was performed to quantify viability of lymphocytes upon absorbed ABT-737 in $Il10^{-/-}$ mice.

The relative number of live peripheral blood lymphocytes (PBL) was reduced significantly in *Il10*$^{-/-}$ upon ABT-737 compared to controls (45·4 ± 17·4%, $n = 8$ *versus* 82·4 ± 4·8%, $n = 8$, respectively, $P < 0·05$, Fig. 1a). Haematological analyses were performed in the *Il10*$^{-/-}$ model of spontaneous colitis to determine whether the significant increase in number of apoptotic cells upon ABT-737 was associated with a shift in cell populations. The lymphocyte fraction was reduced significantly in *Il10*$^{-/-}$ mice after 14 daily injections of ABT-737 when compared to vehicle-receiving controls (45·9 ± 16·1%, $n = 8$ *versus* 67·2 ± 14·0%, $n = 8$, respectively, $P < 0·05$, Fig. 1b). The absolute number of lymphocytes was reduced significantly in *Il10*$^{-/-}$ upon ABT-737 compared to controls (0·53 ± 0·37 × 10^3 cells/μl, $n = 8$ *versus* 1·83 ± 0·83 × 10^3 cells/μl, $n = 8$, respectively, $P < 0·05$). In accordance, the combined granulocyte and monocyte-fraction was increased significantly in ABT-737-treated *Il10*$^{-/-}$ mice (49·3 ± 14·8%, $n = 8$ *versus* 24·6 ± 11·1%, $n = 8$, respectively, $P < 0·05$, Fig. 1c). The absolute number of the combined granulocyte and monocyte-fraction was reduced in *Il10*$^{-/-}$ upon ABT-737 compared to controls (0·54 ± 0·18 × 10^3 cells/μl, $n = 8$ *versus* 0·88 ± 0·48 × 10^3 cells/μl, $n = 8$, respectively), although not significantly different. In contrast, erythrocyte counts were not affected (9·13 ± 0·83 × 10^{12} cells/μl, $n = 8$ *versus* 8·96 ± 0· 87 × 10^{12} cells/μl, $n = 8$). As inhibition of BCL-2 by ABT-737 is mediated by displacing the pro-apoptotic factor BIM, we also applied ABT-737 in *Il10*$^{-/-}$ × *Bim*$^{-/-}$. Both the fraction of lymphocytes (78·8 ± 10·1%, $n = 5$ *versus* 81·2 ± 7·5%, $n = 4$, respectively, Fig· 1b) and of granulocytes and monocytes (10·9 ± 7·8%, $n = 5$ *versus* 12·8 ± 4·3%, $n = 4$, respectively, Fig. 1c) were unaltered upon ABT-737. The absolute number of lymphocytes remained unchanged in *Il10*$^{-/-}$ × *Bim*$^{-/-}$ upon ABT-737 compared to controls (6·16 ± 3·61 × 10^3 cells/μl, $n = 5$ *versus* 5·47 ± 3·81 × 10^3 cells/μl, $n = 5$, respectively), as well as the absolute number of the combined granulocyte and monocyte-fraction (0·90 ± 1·22 × 10^3 cells/μl, $n = 5$ *versus* 1·08 ± 0·71 × 10^3 cells/μl, $n = 5$, respectively). PBL from colitic *Il10*$^{-/-}$ mice were analysed by mass cytometry. T cell receptor (TCR)-β$^+$, CD3$^+$ and CD4$^+$ were analysed for CD44 and CD62L expression (Fig. 1d). The proportion of CD44$^+$CD62L$^+$ central memory T cells was decreased upon ABT-737 (10·4 ± 7·4%, $n = 3$) compared to vehicle-receiving controls (23·8 ± 8·1, $n = 3$). The proportion of TCR-β$^+$, CD3$^+$, CD8$^+$ and CD44$^+$CD62L$^-$ central memory T cells was decreased upon ABT-737 (17·9 ± 11·5%, $n = 3$) compared to vehicle-receiving controls (34·2 ± 24·0, $n = 3$).

Additionally, haematological analyses for C57-BL/6J-Fue mice with a DSS-induced acute colitis confirmed a significantly reduced absolute lymphocyte count upon ABT-737 compared to controls (Supporting information, Fig. S1a). ABT-737 levels in peripheral blood determined by MS were correlated directly to the removal of lymphocytes, as well as an increased relative number of granulocytes and monocytes (Supporting information, Fig. S1c). The absolute number of the combined granulocyte and monocyte-fraction was reduced in mice suffering from DSS-induced colitis upon ABT-737 compared to controls (1·04 ± 0·68 × 10^3 cells/μl, $n = 12$ *versus* 1·42 ± 1·04 × 10^3 cells/μl, $n = 12$, respectively), although not significantly different. In flow cytometry, CD8$^+$ appeared to be diminished upon ABT-737 treatment, although the differences were not significant (7·8 ± 3·2%, $n = 10$ *versus* 10·7 ± 6·2%, $n = 12$, respectively).

The decrease in lymphocyte counts is accompanied by a reduction of proinflammatory cytokines

We determined whether the significant decrease of lymphocyte counts in *Il10*$^{-/-}$ mice was associated with a decrease in *TNF* and *IL1b* gene expression upon ABT-737 treatment. The cytokine profile of *Il10*$^{-/-}$ mice was assessed in peripheral blood drawn from the tail vein on days 7 and 14. *TNF* gene expression was decreased significantly on day 14 in ABT-737-treated mice compared to vehicle-treated mice (82 ± 28, $n = 8$ *versus* 241 ± 15, $n = 8$, respectively, Fig. 2a). *IL1b* gene expression was also decreased significantly on day 14 in ABT-737-treated mice (49 ± 27, $n = 8$ *versus* 276 ± 135, $n = 8$, respectively, Fig. 2b). With regard to *Il6* and *Ifng* mRNA expression, no significant changes were recorded.

BIM is required for the protective effect of ABT-737

Splenocytes from colitis *Il10*$^{-/-}$ mice were analysed by flow cytometry after 14 daily injections of ABT-737. ABT-737 treatment was followed by a significant decrease in CD8$^+$ splenocytes in *Il10*$^{-/-}$ mice compared to vehicle-receiving *Il10*$^{-/-}$ mice (15·9 ± 3·3%, $n = 9$ *versus* 9·2 ± 2·5%, $n = 9$, respectively, $P < 0·05$, Fig. 3a,b). To elucidate ABT-737-dependent changes in apoptosis in the absence of BIM, *Bim*$^{-/-}$ × *Il10*$^{-/-}$ mice were used. In contrast to the results obtained from *Il10*$^{-/-}$ mice, there was no detectable difference in CD8$^+$ splenocytes from *Bim*$^{-/-}$ × *Il10*$^{-/-}$ mice upon ABT-737 (Fig. 3a). This significant decrease in CD3$^+$ CD8$^+$ splenocytes in *Il10*$^{-/-}$ mice upon ABT-737 compared to vehicle-receiving *Il10*$^{-/-}$ mice (17·5 ± 1·1%, $n = 3$ *versus* 11·5 ± 1·9%, $n = 3$, respectively, $P < 0·05$; statistical analysis was performed using the Holm–Sidak method, Fig. 3c) was also confirmed by mass cytometry.

Apoptosis of splenocytes is increased significantly upon ABT-737 treatment

Increased apoptosis in peripheral blood was associated with a reduction of lymphocyte counts in ABT-737-treated mice. The level of cleavage of genomic DNA in spleen in the DSS-induced acute colitis model was

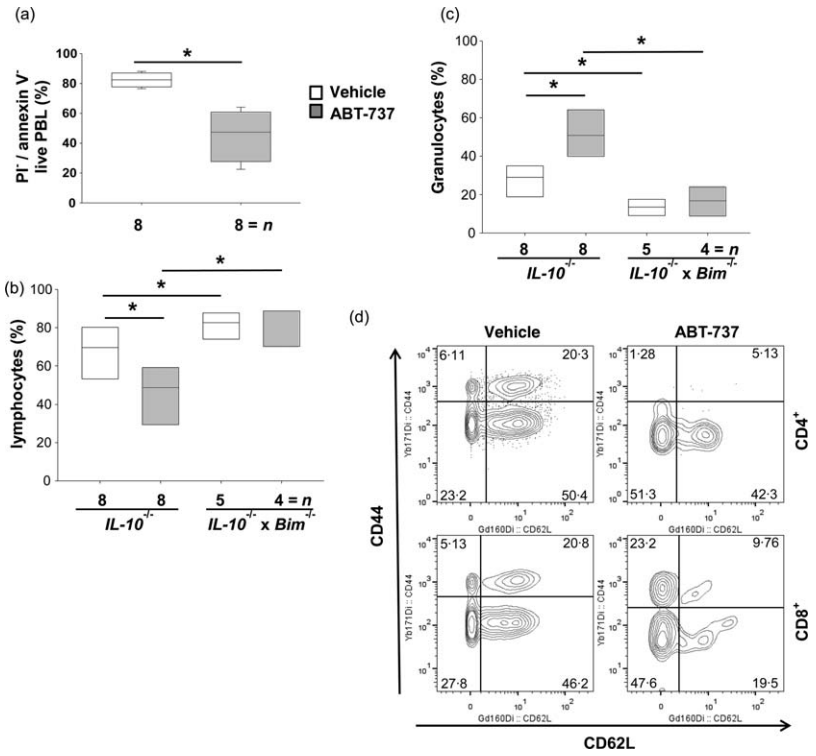

Fig. 1. Cell death upon ABT-737 is selective for peripheral blood (PBL). (a–d) *Il10*$^{-/-}$ and *Il10*$^{-/-}$ × *Bim*$^{-/-}$ mice in the model of spontaneous colitis. (a) Flow cytometry revealed an increased number of propidium iodide (PI)$^{+}$ cells in PBL upon ABT-737 treatment. Mann–Whitney rank-sum test. Treatment with ABT-737 (b) significantly decreased the number of lymphocytes and (c) significantly increased the number of granulocytes compared to vehicle. Statistical analysis was performed using analysis of variance (ANOVA) and all pairwise multiple comparison procedures (Bonferroni *t*-test), $P < 0{\cdot}05$ (*). (d) Mass cytometry revealed a decreased proportion of CD44^{+} CD62L^{+} central memory T cells upon ABT-737 compared to vehicle.

analysed. TUNEL assays revealed an increased apoptosis in mice treated for 9 days with ABT-737 (Supporting information, Fig. S2a,b). Apoptosis-positive cells were detectable in the red pulp and to a lesser extent in the white pulp.

Furthermore, ABT-737 treatment was followed by a significant reduction in spleen weight in C57-BL/6J-Fue mice suffering from DSS-induced acute colitis ($0{\cdot}10 \pm 0{\cdot}03$ g for vehicle-receiving mice compared to $0{\cdot}07 \pm 0{\cdot}02$ g for ABT-737-receiving mice; Supporting information, Fig. S2c,d). This difference in spleen weight was not seen in colitic *Bim*$^{-/-}$ mice upon ABT-737 treatment. Irrespective of the treatment, spleen weight in *Bim*$^{-/-}$ was increased compared to C57-BL/6J-Fue mice, as described previously (Supporting information, Fig. S2c).

ABT-737 increases apoptosis significantly in Peyer's patches

The increased number of TUNEL^{+} cells in the peripheral blood and spleen indicated that the number of lymphocytes was reduced in ABT-737-treated mice. Additionally, significantly increased cleavage of genomic DNA was found in Peyer's patches in the *Il10*$^{-/-}$ model in both groups treated for 5 (Supporting information, Fig. S3a) and 14 days (Fig. 4a,b) with ABT-737. Next we isolated LPMNC from small bowel from *Il10*$^{-/-}$ treated for 14 days. Viable cells were identified by cisplatin staining followed by mass cytometry. A certain number of dead cells is certainly due to the isolation procedure; however, a significantly increased number of dead cells was found in LPMNC isolated from small bowel in the *Il10*$^{-/-}$ model with ABT-737 compared to vehicle-treated mice ($72{\cdot}9 \pm 3{\cdot}1\%$, $n = 3$ *versus* $46{\cdot}8 \pm 12{\cdot}2\%$, $n = 3$, respectively, $P < 0{\cdot}05$, Holm–Sidak method, Fig. 4c). A decrease in viable CD3^{+}CD4^{+} LPMNC in *Il10*$^{-/-}$ mice upon ABT-737 compared to vehicle-receiving *Il10*$^{-/-}$ mice ($4{\cdot}9 \pm 3{\cdot}8\%$, $n = 3$ *versus* $13{\cdot}3 \pm 6{\cdot}4\%$, $n = 3$, respectively, $P < 0{\cdot}05$, Fig. 4d) was confirmed by mass cytometry. Additionally, a decrease in viable CD3^{+}CD8^{+} LPMNC upon ABT-737 ($3{\cdot}6 \pm 2{\cdot}7\%$, $n = 3$ *versus* $11{\cdot}2 \pm 6{\cdot}4\%$, $n = 3$, respectively, $P < 0{\cdot}05$, Fig. 4d) was found.

Although mice suffering from acute DSS-induced colitis do not develop ileitis, TUNEL staining also revealed increased apoptosis in Peyer's patches from mice treated

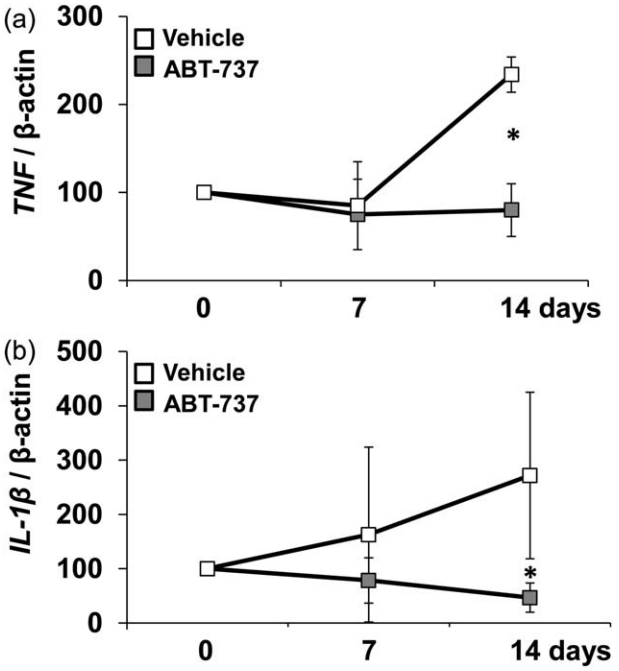

Fig. 2. During spontaneous colitis in interleukin (IL)-$10^{-/-}$ proinflammatory cytokines were decreased significantly upon ABT-737 treatment compared to vehicle-receiving controls. mRNA expression levels determined by quantitative polymerase chain reaction (qPCR) from (a) tumour necrosis factor (TNF) and (b) IL-1b. Statistical analysis was performed using the Mann–Whitney rank-sum test, $P < 0{\cdot}05$ (*).

for 9 days with ABT-737 upon water (Supporting information, Fig. S4) or DSS (Supporting information, Fig. S5). TUNEL also revealed an increased apoptosis in the lamina propria of mice treated for 9 days with ABT-737 (Supporting information, Figs S4 and S5). TUNEL$^+$ cells appeared more frequently as clusters of more than four cells (Supporting information, Fig. S6).

ABT-737 ameliorates spontaneous and acute colitis

To determine the influence of ABT-737 dependent on mucosal inflammation and apoptosis both the *Il10*$^{-/-}$ model and the DSS-induced model were used. Macroscopic mucosal damage was assessed by mini-endoscopy. *Il10*$^{-/-}$ mice with a clearly visible rectal prolapse received 50 mg/kg/day ($n = 18$) or vehicle ($n = 14$) for 14 days. Mice were killed on day 14. *Il10*$^{-/-}$ mice receiving vehicle displayed an opaque mucosa and altered vascular pattern on day 14 (MEICS $6{\cdot}9 \pm 2{\cdot}3$, $n = 14$, Fig. 5a). The thickening of the colon became more prominent, thin faeces were discovered and the diseased regions presented frequently with mucosal bleeding. During treatment with ABT-737, inflammation was ameliorated. Compared to vehicle-receiving mice, *Il10*$^{-/-}$ mice treated with ABT-737 had a transparent mucosa with a regular vascular pattern. Solid faeces were visible (MEICS $3{\cdot}6 \pm 1{\cdot}7$, $n = 18$, Fig. 5b). No differences in MEICS were determined in *Il10*$^{-/-}$ × *Bim*$^{-/-}$ upon ABT-737 (Fig. 5a,b).

Additionally, upon acute colitis, mice receiving vehicle displayed an opaque mucosa and altered vascular pattern on day 9 (MEICS $4{\cdot}3 \pm 1{\cdot}8$, $n = 14$; Supporting information, Fig. S7). Colon became thickened, extensive amounts of faeces were discovered and the diseased regions presented frequently with mucosal bleeding. During treatment with ABT-737 signs of an ameliorated inflammation were found. Mice suffering from DSS-induced acute colitis but treated with ABT-737 had a transparent mucosa with a regular vascular pattern. Solid faeces were visible (MEICS $1{\cdot}4 \pm 0{\cdot}9$, $n = 13$; Supporting information, Fig. S7). In contrast, no difference in MEICS

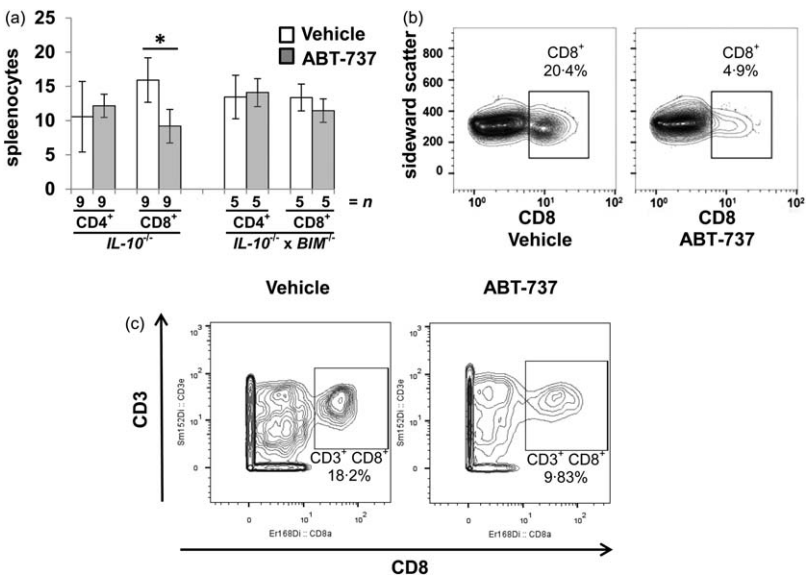

Fig. 3. Increased apoptosis in the spleen upon ABT-737 treatment. (a–c) Interleukin (IL)-$10^{-/-}$ mice suffering from spontaneous colitis. (a) Decreased number of CD8$^+$ splenocytes in *Il10*$^{-/-}$ upon ABT-737 compared to vehicle determined by flow cytometry. Number of CD4$^+$ and CD8$^+$ splenocytes in *Bim*$^{-/-}$ × *Il10*$^{-/-}$ remained unchanged upon ABT-737. Statistical analysis was performed using the Mann–Whitney rank-sum test, $P < 0{\cdot}05$ (*). (b) Decreased number of CD8$^+$ splenocytes in *Il10*$^{-/-}$ upon ABT-737 compared to vehicle determined by flow cytometry. (c) Mass cytometric analysis of T cell receptor (TCR)β$^+$ splenocytes revealed a significantly decreased proportion of CD3$^+$CD8$^+$ T cells upon ABT-737 compared to vehicle. Statistical analysis was performed using the Holm–Sidak method, $P < 0{\cdot}05$ (*).

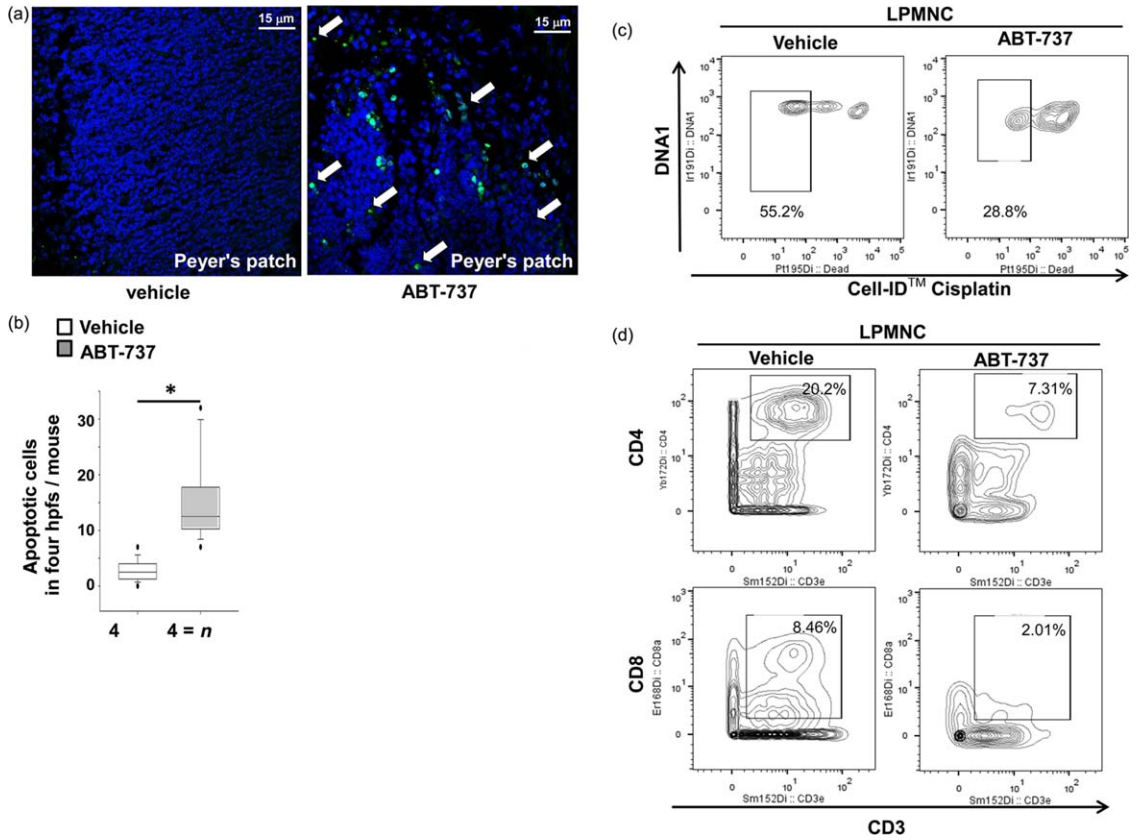

Fig. 4. Increased number of terminal deoxynucleotidyl transferase dUTP nick end labelling $(TUNEL)^+$ cells in Peyer's patches of the small bowel upon ABT-737. (a) $Il10^{-/-}$ mice were killed at day 14; original magnification × 630. Statistical analysis was performed using the Mann–Whitney rank-sum test, $P < 0{\cdot}05$ (*). (b) The number of cells was calculated from four high-power fields for each mouse. (c) Mass cytometric analysis of of lamina propria mononuclear cells (LPMNC) revealed a significant decrease in dead cells upon ABT-737 compared to vehicle. Statistical analysis was performed using the Holm–Sidak method, $P < 0{\cdot}05$ (*). (d) Mass cytometric analysis LPMNC revealed a decrease in both $CD3^+CD4^+$ and $CD3^+CD8^+$ T cells upon ABT-737 compared to vehicle.

was determined in $Bim^{-/-}$ mice treated with ABT-737 (Supporting information, Fig. S7). In summary, ABT-737 positively altered the colonic mucosa at a macroscopic level in both the $Il10^{-/-}$ model of spontaneous colitis and DSS-induced acute colitis.

Colon length was determined in both spontaneous colitis and DSS-induced acute colitis models. In $Il10^{-/-}$ mice, ABT-737 treatment prevented the shortening in colon length significantly ($8{\cdot}18 \pm 0{\cdot}27$ cm *versus* $7{\cdot}65 \pm 0{\cdot}38$ cm, respectively, Fig. 6a). The histological

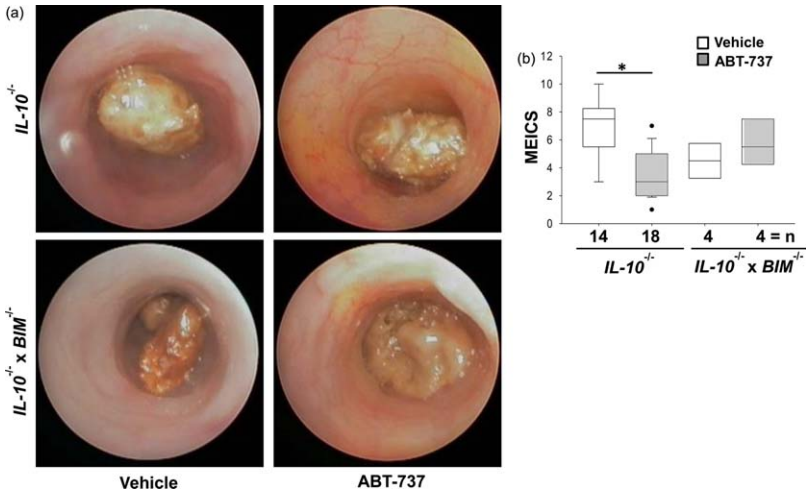

Fig. 5. Mice suffering from colitis develop an ameliorated intestinal inflammation upon ABT-737 treatment compared to vehicle-receiving mice. (a,b) $Il10^{-/-}$ mice suffering from spontaneous colitis. (a) Representative images demonstrate colonoscopy pictures derived from ABT-737- and vehicle-treated mice. (b) Statistical analysis of colonoscopy score [murine endoscopic index of colitis severity (MEICS)]. Normality test was passed and statistical analysis was performed using one way analysis of variance (ANOVA) (Bonferroni *t*-test). Colonoscopy was performed on the day prior to killing the animals. Box-plots express median, 95/5% percentiles and outliers, $P < 0{\cdot}05$ (*).

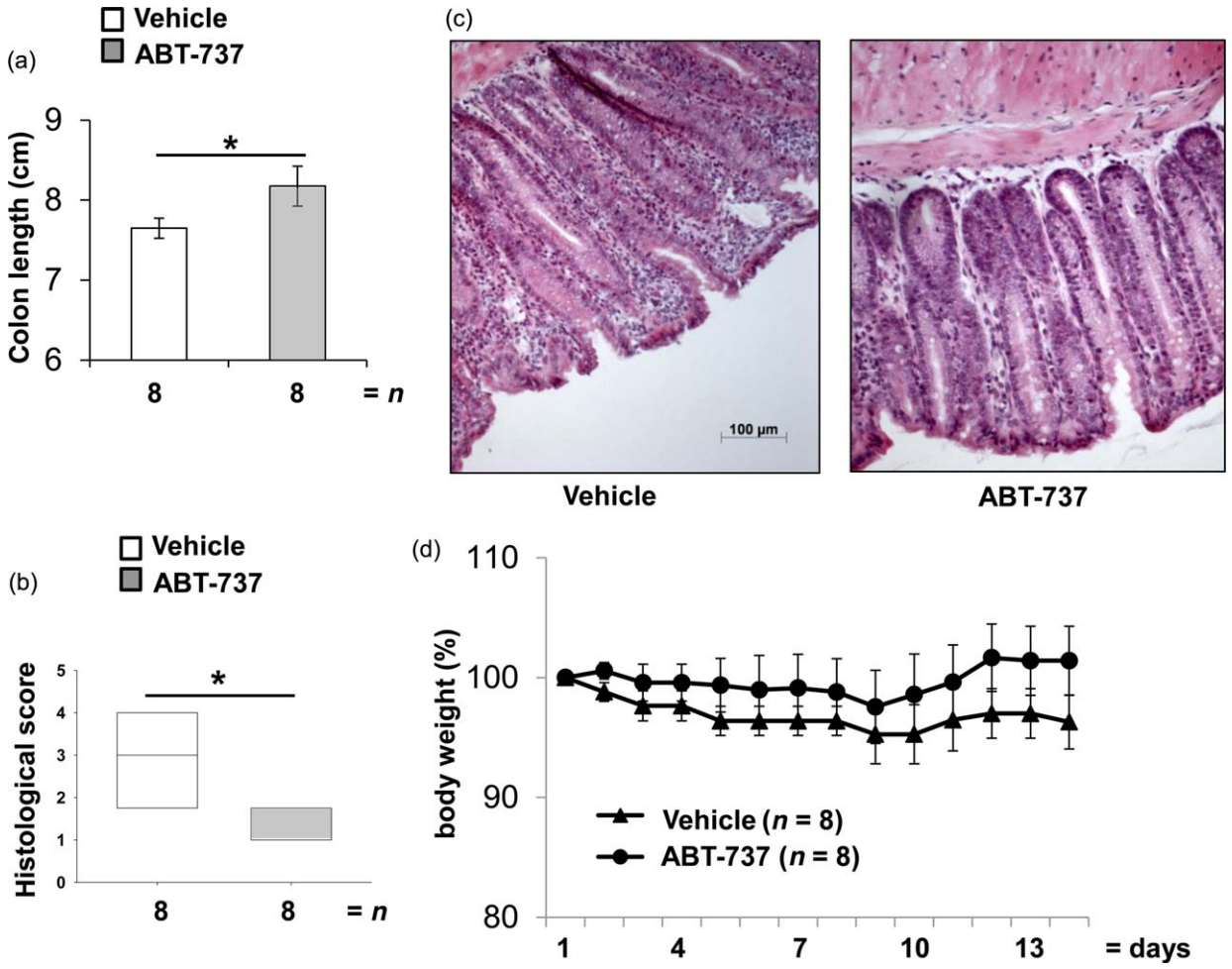

Fig. 6. ABT-737 treatment was followed by a significant increase of the colon length. (a–d) *Il10*$^{-/-}$ mice suffering from spontaneous colitis. (a) In *Il10*$^{-/-}$ mice ABT-737 treatment was followed by a significant increase in colon length. Statistical analysis was performed using the Mann–Whitney rank-sum test. (b) Histological score was decreased significantly upon ABT-737 treatment. Statistical analysis was performed using the Mann–Whitney rank-sum test. Box-plots express median. (c) Haematoxylin and eosin (H&E) staining of distal colon. Images representative for n = eight each, $P < 0{\cdot}05$ (*); $P < 0{\cdot}001$ (***). (d) Body weight curve.

score of *Il10*$^{-/-}$ mice treated with ABT-737 was significantly lower, as in untreated mice (Fig. 6b). ABT-737-treated *Il10*$^{-/-}$ mice had less lymphocyte influx in the thickened lamina propria (Fig. 6c). Compared to vehicle-receiving mice, *Il10*$^{-/-}$ mice treated with ABT-737 showed increased body weight (Fig. 6d), although not significantly different.

In C57-BL/6J-Fue mice, induction of DSS-induced acute colitis was followed by a significant reduction in colon length (Supporting information, Fig. S8a). ABT-737 treatment prevented the shortening in colon length significantly in DSS-induced colitis ($7{\cdot}44 \pm 0{\cdot}51$ cm, $n = 18$ *versus* $6{\cdot}35 \pm 0{\cdot}57$ cm, $n = 18$, $P < 0{\cdot}001$, respectively; Supporting information, Fig. S8a). The number of lymphocytes in colonic mucosa was determined and immunohistochemistry applying anti-CD3 antibody was performed. CD3$^+$ cells in the acquired images were marked appropriately and quantified by an investigator blinded to the experiment setup. Immunohistochemistry revealed a decreased number of CD3$^+$ in the colonic lamina propria of mice treated for 9 days with ABT-[$49{\cdot}5 \pm 39{\cdot}5$ cells/high-power field (hpf), $n = 16$ hpfs and $70{\cdot}1 \pm 30{\cdot}4$ cells/hpf, $n = 14$ hpfs, respectively; Supporting information, Fig. S8b].

CD4$^+$CD62L$^+$ are susceptible for priming with ABT-737 but *Bcl-2* increases during ongoing inflammation

We assessed ABT-737-dependent priming for apoptosis in lymphocyte subpopulations. *Il10*$^{-/-}$ with a clearly visible rectal prolapse received either a dose of 50 mg/kg/day ABT-737 ($n = 5$) or vehicle ($n = 5$) for 14 days as *in-vivo* pretreatment. CD4$^+$CD62L$^+$ were isolated from the splenocytes and incubated for 12 h with ABT-737 or vehicle. Following ABT-737 *in-vivo* pretreatment CD4$^+$CD62L$^+$ cells became significantly more susceptible to apoptosis

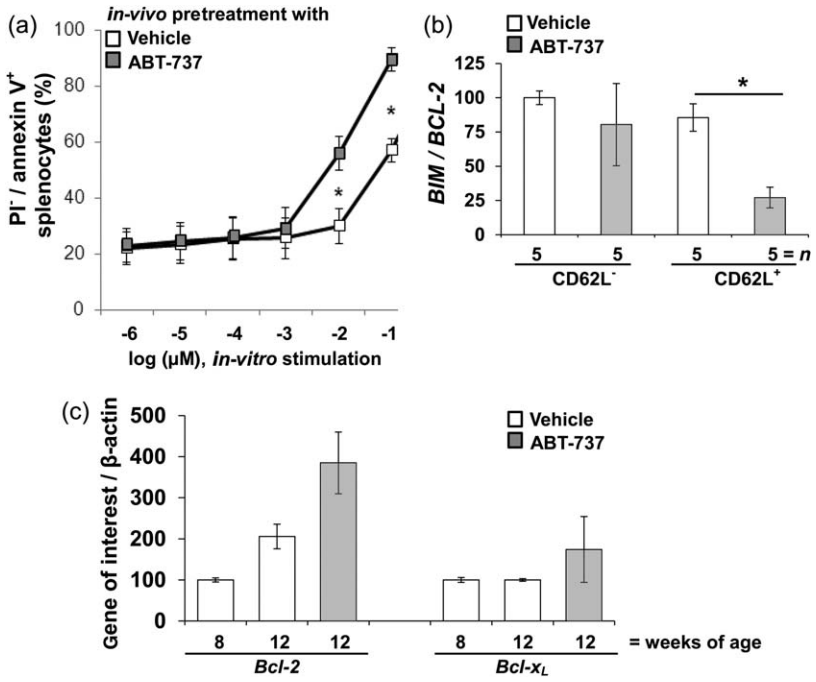

Fig. 7. Significantly increased apoptosis in $CD4^+CD62L^+$ from $Il10^{-/-}$ mice upon ABT-737 pretreatment compared to vehicle. (a) $CD4^+CD62L^+$ cells were isolated from $Il10^{-/-}$ mice treated for 14 days with ABT-737 or vehicle *in vivo*. $CD4^+CD62L^+$ cells were stimulated *in vitro* with ABT-737 or vehicle in a dose-dependent manner. Following ABT-737 pretreatment, cells became significantly more susceptible to the initiation of apoptosis as determined by flow cytometry. (b) The *BIM/BCL-2* ratio was decreased significantly in $CD4^+CD62L^+$ from ABT-737-treated mice compared to vehicle-treated mice. (c) BCL-*2* and *BCL-*x_L quantitative polymerase chain reaction (qPCR) of splenocytes isolated from $Il10^{-/-}$. Gene expression was increased in a time-dependent manner and upon ABT treatment compared to vehicle-receiving controls. Statistical analysis was performed using the Mann–Whitney rank-sum test, $P < 0{\cdot}05$ (*).

initiated by ABT-737 compared to vehicle controls (Fig. 7a). According contour plots are shown in Supporting information, Fig. S9.

Furthermore, *BIM* and *BCL-2* gene expression in $CD4^+CD62L^+$ and $CD4^+CD62L^-$ cells after pretreatment with either ABT-737 or vehicle was determined. The *BIM*/*BCL-2* ratio was decreased significantly on day 14 in $CD4^+CD62L^+$ from ABT-737-treated mice compared to vehicle-treated mice (26 ± 8, $n = 5$ *versus* 87 ± 13, $n = 5$, respectively, Fig. 7b). *In-vivo* pretreatment with ABT-737 lowered the *BIM*/*BCL-2* ratio in $CD4^+CD62L^+$. As the *BIM*/*BCL-2* ratio was decreased significantly on day 14 in $CD4^+CD62L^+$ from ABT-737-treated mice, *BCL-2* and *BCL-XL* gene expression in $CD4^+CD62L^+$ cells in relation to age and treatment was determined. $CD4^+CD62L^+$ from IL-$10^{-/-}$ 8 weeks of age ($n = 5$) were compared to 12-week-old mice with ($n = 5$) and without ABT-737 treatment ($n = 5$). Eight-week-old mice without visible rectal prolapse were compared with 12-week-old mice with either a visible or a developing rectal prolapse. *BCL-2* gene expression was increased significantly in older mice compared to younger mice. *BCL-2* was also increased significantly upon ABT-737 compared to vehicle control (Fig. 7c).

Apoptosis stimulating effect is decreased upon ABT-737 long-term treatment

Long-term treatment with ABT-737 in $Il10^{-/-}$ mice was performed. $Il10^{-/-}$ at 8 weeks of age, with no signs of rectal prolapse, received either 50 mg/kg ABT-737 every 3 days ($n = 10$) or vehicle ($n = 10$) during a period of 56 days. Treatment was applied i.p. Long-term treatment with ABT-737 induced depigmentation of the abdominal skin, whereas the head, chest and back were not affected (Supporting information, Fig. S10).

$Il10^{-/-}$ were killed on day 56. Seven mice upon ABT-737 and eight vehicle-treated mice developed a clearly visible rectal prolapse during the experiment. Macroscopic mucosal damage was assessed by mini-endoscopy and colonoscopy score on days 14 and 55. On day 55 $Il10^{-/-}$ mice from both groups displayed an opaque mucosa and altered vascular pattern (Fig. 8a). The thickening of the colon became more prominent, thin faeces were discovered and the diseased regions presented frequently with mucosal bleeding (MEICS $10{\cdot}0 \pm 2{\cdot}5$, $n = 5$ for mice devoid of ABT-737 compared to $11{\cdot}1 \pm 2{\cdot}9$, $n = 5$ for mice upon ABT-737, Fig. 8b).

The cytokine profile in peripheral blood was assessed on days 0, 14, 28, 42 and 56 without further prestimulation of lymphocytes at mRNA level (Fig. 8c). In support of data from the short time-frame experiments mentioned above, *TNF* gene expression was decreased significantly on day 14 in ABT-737-treated mice compared to vehicle-treated mice. No significant changes were recorded between treatment with ABT-737 and vehicle on day 56.

Discussion

As dysregulated apoptosis of activated lymphocytes driven by increased anti-apoptotic BCL-2 and BCL-XL contributes to the pathogenesis of IBD [3,4,6,7,32], we analysed the potential of the priming agent ABT-737 to limit the persistence of lymphocytes in mouse models of colitis.

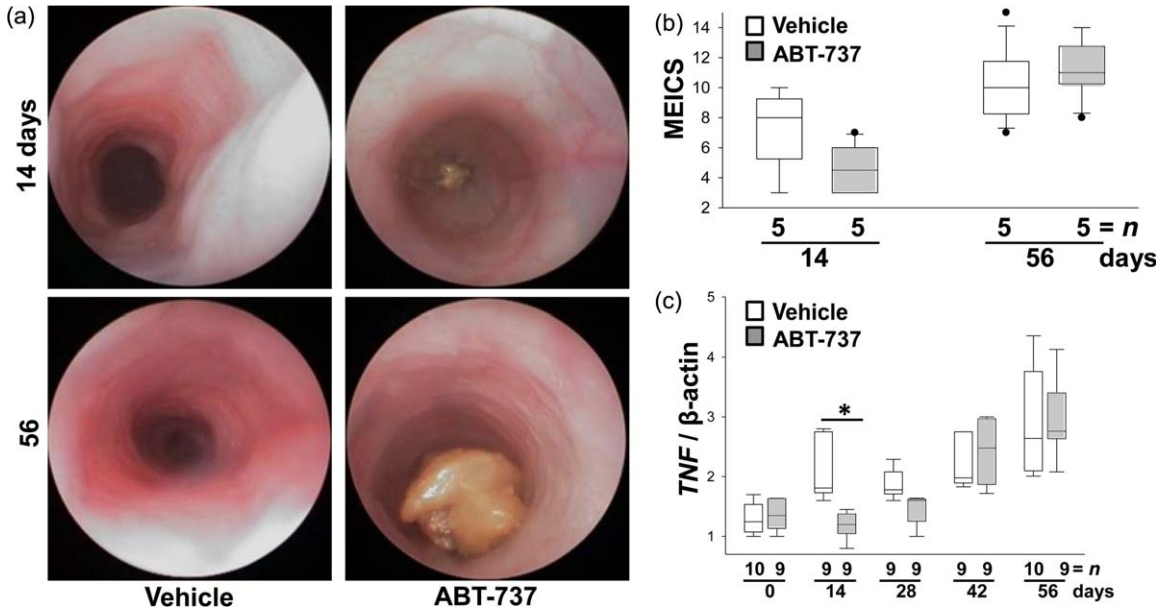

Fig. 8. During long-term treatment interleukin (IL)-$10^{-/-}$ mice develop intestinal inflammation despite ABT-737 application (50 mg/kg/3 days for 14 and 56 days), similar to vehicle-receiving mice. (a) Representative images demonstrate colonoscopy pictures derived from ABT-737- and vehicle-treated IL-$10^{-/-}$ mice. (b) Statistical analysis of colonoscopy score [murine endoscopic index of colitis severity (MEICS)]. Colonoscopy was performed on days 14 and 56 (1 day prior to killing the animals). Box-plots express median, 95/5% percentiles and outliers. (c) The cytokine profile of peripheral blood lymphocytes isolated from IL-$10^{-/-}$ is altered in a time-dependent manner upon ABT-737 treatment compared to vehicle controls. Tumour necrosis factor (TNF) mRNA expression levels determined by quantitative polymerase chain reaction (qPCR). Statistical analysis was performed using the Mann–Whitney rank-sum test, $P < 0{\cdot}05$ (*).

In the present study, we applied pro-apoptotic ABT-737 in both the murine model of acute DSS-induced colitis and the *Il10*$^{-/-}$ model of spontaneous colitis. Following i.p. administration, ABT-737 was detected in peripheral blood, colon tissue and IEC. We determined ABT-737 accumulation in the faeces. ABT-737 treatment led to lymphopenia in mice, demonstrated by the reduced lymphocyte and thrombocyte counts as well as the increased fraction of combined granulocytes and monocytes compared to controls. PBL were cleared in a dose-dependent manner upon ABT-737 and proportions of $CD8^+$ appeared to be diminished. Increased apoptosis upon ABT-737 was determined in PBL, splenocytes and Peyer's patches and was accompanied by a decrease in *TNF* and *IL1b* gene expression compared to vehicle control. $CD4^+CD44^+CD62L^+$ central memory T cells were decreased in PBL upon ABT-737 compared to vehicle-receiving controls. $CD8^+$ and $CD44^+CD62L^-$ central memory T cells were also decreased upon ABT-737. Naive T cells require both MCL-1 and BCL-2 for survival (Ivan Dzhagalov *et al.*) [33]. In our own experiments, $CD4^+$ naive T cells are hardly affected by ABT-737, which is not inhibiting MCL-1. This may protect T cell subpopulations from initiation of apoptosis and contribute to a low *BIM/BCL-2* ratio in the remaining cells. ABT-737 positively alters the colonic mucosa at both macroscopic and microscopic levels, while also ameliorating intestinal inflammation in models of colitis, as shown by MEICS, histological score and colon length. Inactivation of BCL-2 is key to the ability of BIM to induce apoptosis. BIM can also bind directly to pro-apoptotic BAX and BAK in order to initiate apoptosis [34]. Other BH3-only proteins such as BMF, BAD, NOXA and PUMA are considered to act as sensitizers which bind the prosurvival BCL-2 protein and thereby displace BIM from BCL-2 to promote cell death [35]. As inhibition of BCL-2 by ABT-737 is mediated by BIM, we also applied ABT-737 to both *Il10*$^{-/-}$ × *Bim*$^{-/-}$ upon spontaneous colitis and *Bim*$^{-/-}$ upon DSS-induced acute colitis and confirmatively mice were found to be relatively resistant to the lymphocyte apoptosis upon ABT-737 administration. In our own experiments we could also show that following 14 days of ABT-737 pre-treatment *in vivo*, gut-homing $CD4^+CD62L^+$ cells became more susceptible to apoptosis compared to vehicle controls. *BIM/BCL-2* balance is critical for maintaining T cell homeostasis [9]. However, the *BIM/BCL-2* ratio was decreased with age and during the course of treatment in our own experimental setup. Thus, long-term treatment for a period of 56 days resulted in adapted *TNF* levels and macroscopic mucosal damage.

ABT-737 affects various transformed cells, while exhibiting minimal toxicity toward normal cells. Navitoclax, the orally administered form of ABT-737, has been applied in chronic lymphocytic leukaemia (CLL). CLL is

characterized by the accumulation of lymphocytes, typically of B cell origin, in the blood, lymph nodes and spleen. In a Phase I study of 26 patients, nine achieved a partial response and seven maintained stable disease for more than 6 months [36]. Furthermore, the expression of Bim, and the extent of its association with Bcl-2, correlates with *in-vivo* ABT-737 sensitivity in CLL [27]. Navitoclax has also been tested successfully in small cell lung cancer xenograft models. Although navitoclax exhibited an important range of anti-tumour activity, leading to complete tumour regression in several models [37], Bcl-2 targeting by navitoclax showed limited single-agent activity against advanced and recurrent small cell lung cancer in a Phase II study [38].

Studies observing ABT-737 in inflammatory conditions characterized by the uncontrolled proliferation of lymphocytes yielded results which corroborated our own findings. ABT-737 was efficacious in reducing accumulated lymphocytes associated with tissue and organ damage in other animal models of autoimmunity. Collagen-induced arthritis in DBA/J mice is a well-established rodent model for rheumatoid arthritis, which is characterized clinically by paw swelling leading to ankylosis. Treatment with ABT-737 and dexamethasone reduced the mean arthritic score and paw swelling significantly compared with the vehicle-treated group [24]. ABT-737 treatment was associated with lymphocyte and platelet depletion. In parallel, ABT-737 was applied in a murine model of delayed-type hypersensitivity (DTH) in C57BL/6 mice. The DTH test is used to determine whether a previous exposure to a specific antigen has occurred. This reaction has been shown to be dependent upon $CD4^+$ and $CD8^+$ memory T cells. Treatment with ABT-737 and dexamethasone showed a similar reduction in paw swelling compared to the vehicle-treated group [24]. ABT-737 was also applied in a murine model of interferon (IFN)-γ-induced lupus nephritis. Treatment with ABT-737 prolonged survival and reduced glomerulonephritis to a similar extent to that observed with mycophenolate mofetil [24]. In animal models of systemic lupus erythematosus, a decrease in lymphocyte apoptosis is associated clearly with more severe disease pathogenesis. Both Bcl-2-transgenic mice [39] and BIM-deficient mice [40] show evidence of systemic lupus erythematosus-like clinical symptoms caused by prolonged survival of lymphocytes. In patients with lupus, elevated Bcl-2 expression in lymphocytes has been reported [41].

The regulative function of ABT-737 on uncontrolled proliferation of lymphocytes could also be confirmed with a different approach. ABT-737 suppresses allogeneic T and B cell responses after skin transplantation [42]. *In vitro*, ABT-737 prevented allogeneic T cell activation, proliferation and cytotoxicity by inducing apoptosis. The physiological functions of the remaining viable T cells were not impaired. *In vivo*, ABT-737 was highly selective for lymphoid cells and inhibited allogeneic T and B cell responses after skin transplantation.

In recent years the importance of expansion and contraction of activated lymphocytes by apoptosis has been discussed extensively. Failure in the apoptotic mechanism of lymphocyte control can lead to the development of autoimmunity. Inducing the apoptosis of lymphocytes may provide the basis for a new therapeutic strategy in CD patients. Furthermore, investigating the imbalance between pro-and anti-apoptotic proteins could help to predict clinical relapse upon standard medical therapy. Ultimately, this knowledge could lead to the development of new therapeutic options for the treatment of IBD by focusing on controlling the abnormally large population of activated cells and thereby restoring a physiological turnover of lymphocytes and homeostasis.

Acknowledgements

We thank Professor Dr Thomas Fehr (Division of Nephrology, University Hospital Zurich, Switzerland) for providing ABT-737, murine intestinal tissue and invaluable help with the start-up of the project. This research was supported by grant IBD-0324R from the Broad Medical Research Foundation (BMRF) to M. H. This research was also supported by grant Project no. 2013-16 from the Swiss inflammatory bowel disease cohort study (SIBDCS) to M. H. and by grant Project no. 314730_152895/1 from the Swiss National Science Foundation.

Disclosure

C. L., M. M., V. T., M. C., P. C., M. F. and M. H. have no conflicts of interest to disclose. G. R. discloses grant support from AbbVie, Ardeypharm, MSD, FALK, Flamentera, Novartis, Roche, Tillots, UCB and Zeller. B. L. M. and C. L. G. are employees of AbbVie. B. L. M. and C. L. G. provided ABT-737, performed MS analysis and further contributed to the discussion of the data; however, AbbVie did not provide any additional financial support (e.g. writing/editing of the manuscript).

Author contributions

For the study concept: M. H.; for acquisition of the data: C. L., M. M., V. T., M. C., B. L. M., C. L. G. and M. H.; for critical revision of the manuscript: C. L., P. C., B. L. M., C. L. G., M. F. and G. R.

References

1 Mitchell T, Kappler J, Marrack P. Bystander virus infection prolongs activated T cell survival. J Immunol 1999; **162**:4527–35.

2 Hildeman DA, Zhu Y, Mitchell TC et al. Activated T cell death *in vivo* mediated by proapoptotic bcl-2 family member bim. Immunity 2002; **16**:759–67.

3 Boirivant M, Marini M, Di Felice G et al. Lamina propria T cells in Crohn's disease and other gastrointestinal inflammation show defective CD2 pathway-induced apoptosis. Gastroenterology 1999; **116**:557–65.

4 Ina K, Itoh J, Fukushima K et al. Resistance of Crohn's disease T cells to multiple apoptotic signals is associated with a Bcl-2/Bax mucosal imbalance. J Immunol 1999; **163**:1081–90.

5 Itoh J, de La Motte C, Strong SA, Levine AD, Fiocchi C. Decreased Bax expression by mucosal T cells favours resistance to apoptosis in Crohn's disease. Gut 2001; **49**:35–41.

6 Atreya R, Mudter J, Finotto S et al. Blockade of interleukin 6 trans signaling suppresses T-cell resistance against apoptosis in chronic intestinal inflammation: evidence in Crohn disease and experimental colitis *in vivo*. Nat Med 2000; **6**:583–8.

7 Iborra M, Moret I, Buso E et al. Differential regulation of oxidative stress and apoptosis related genes during active and inactive Crohn's disease (CD). Gastroenterology 2012; **142** (Suppl. 1):S–877.

8 Veltkamp C, Anstaett M, Wahl K et al. Apoptosis of regulatory T lymphocytes is increased in chronic inflammatory bowel disease and reversed by anti-TNFalpha treatment. Gut 2011; **60**:1345–53.

9 Wojciechowski S, Tripathi P, Bourdeau T et al. Bim/Bcl-2 balance is critical for maintaining naive and memory T cell homeostasis. J Exp Med 2007; **204**:1665–75.

10 Bouillet P, Metcalf D, Huang DC et al. Proapoptotic Bcl-2 relative Bim required for certain apoptotic responses, leukocyte homeostasis, and to preclude autoimmunity. Science 1999; **286**:1735–8.

11 Tischner D, Woess C, Ottina E, Villunger A. Bcl-2-regulated cell death signalling in the prevention of autoimmunity. Cell Death Dis 2010; **1**:e48.

12 Dignass A, Lindsay JO, Sturm A et al. Second European evidence-based consensus on the diagnosis and management of ulcerative colitis part 2: current management. J Crohns Colitis 2012; **6**:991–1030.

13 Dignass A, Van Assche G, Lindsay JO et al. The second European evidence-based consensus on the diagnosis and management of Crohn's disease: current management. J Crohns Colitis 2010; **4**:28–62.

14 Doering J, Begue B, Lentze MJ et al. Induction of T lymphocyte apoptosis by sulphasalazine in patients with Crohn's disease. Gut 2004; **53**:1632–8.

15 Bianchi M, Meng C, Ivashkiv LB. Inhibition of IL-2-induced Jak-STAT signaling by glucocorticoids. Proc Natl Acad Sci USA 2000; **97**:9573–8.

16 Steel AW, Mela CM, Lindsay JO, Gazzard BG, Goodier MR. Increased proportion of CD16(+) NK cells in the colonic lamina propria of inflammatory bowel disease patients, but not after azathioprine treatment. Aliment Pharmacol Ther 2011; **33**:115–26.

17 Ben-Horin S, Goldstein I, Fudim E et al. Early preservation of effector functions followed by eventual T cell memory depletion: a model for the delayed onset of the effect of thiopurines. Gut 2009; **58**:396–403.

18 Tiede I, Fritz G, Strand S et al. CD28-dependent Rac1 activation is the molecular target of azathioprine in primary human CD4+ T lymphocytes. J Clin Invest 2003; **111**:1133–45.

19 ten Hove T, van Montfrans C, Peppelenbosch MP, van Deventer SJ. Infliximab treatment induces apoptosis of lamina propria T lymphocytes in Crohn's disease. Gut 2002; **50**:206–11.

20 Lugering A, Schmidt M, Lugering N, Pauels HG, Domschke W, Kucharzik T. Infliximab induces apoptosis in monocytes from patients with chronic active Crohn's disease by using a caspase-dependent pathway. Gastroenterology 2001; **121**:1145–57.

21 Atreya R, Zimmer M, Bartsch B et al. Antibodies against tumor necrosis factor (TNF) induce T-cell apoptosis in patients with inflammatory bowel diseases via TNF receptor 2 and intestinal CD14(+) macrophages. Gastroenterology 2011; **141**:2026–38.

22 Oltersdorf T, Elmore SW, Shoemaker AR et al. An inhibitor of Bcl-2 family proteins induces regression of solid tumours. Nature 2005; **435**:677–81.

23 Chen S, Dai Y, Pei XY, Grant S. Bim upregulation by histone deacetylase inhibitors mediates interactions with the Bcl-2 antagonist ABT-737: evidence for distinct roles for Bcl-2, Bcl-xL, and Mcl-1. Mol Cell Biol 2009; **29**:6149–69.

24 Bardwell PD, Gu J, McCarthy D et al. The Bcl-2 family antagonist ABT-737 significantly inhibits multiple animal models of autoimmunity. J Immunol 2009; **182**:7482–9.

25 Liu H, Pope RM. The role of apoptosis in rheumatoid arthritis. Curr Opin Pharmacol 2003; **3**:317–22.

26 Nagy G, Koncz A, Perl A. T- and B-cell abnormalities in systemic lupus erythematosus. Crit Rev Immunol 2005; **25**:123–40.

27 High LM, Szymanska B, Wilczynska-Kalak U et al. The Bcl-2 homology domain 3 mimetic ABT-737 targets the apoptotic machinery in acute lymphoblastic leukemia resulting in synergistic *in vitro* and *in vivo* interactions with established drugs. Mol Pharmacol 2010; **77**:483–94.

28 Leucht K, Caj M, Fried M, Rogler G, Hausmann M. Impaired removal of Vbeta8 lymphocytes aggravates colitis in mice deficient for BIM. Clin Exp Immunol 2013; **173**:493–501.

29 Becker C, Fantini MC, Wirtz S et al. *In vivo* imaging of colitis and colon cancer development in mice using high resolution chromoendoscopy. Gut 2005; **54**:950–4.

30 Obermeier F, Kojouharoff G, Hans W, Scholmerich J, Gross V, Falk W. Interferon-gamma (IFN-gamma)- and tumour necrosis factor (TNF)-induced nitric oxide as toxic effector molecule in chronic dextran sulphate sodium (DSS)-induced colitis in mice. Clin Exp Immunol 1999; **116**:238–45.

31 Steidler L, Hans W, Schotte L et al. Treatment of murine colitis by *Lactococcus lactis* secreting interleukin-10. Science 2000; **289**:1352–5.

32 Kruidenier L, Kuiper I, Van Duijn W et al. Imbalanced secondary mucosal antioxidant response in inflammatory bowel disease. J Pathol 2003; **201**:17–27.

33 Dzhagalov I, Dunkle A, He YW. The anti-apoptotic Bcl-2 family member Mcl-1 promotes T lymphocyte survival at multiple stages. J Immunol 2008; **181**:521–8.

34 Ewings KE, Wiggins CM, Cook SJ. Bim and the pro-survival Bcl-2 proteins: opposites attract, ERK repels. Cell Cycle 2007; **6**:2236–40.

35 Kutuk O, Letai A. Displacement of Bim by Bmf and Puma rather than increase in Bim level mediates paclitaxel-induced apoptosis in breast cancer cells. Cell Death Differ 2010; **17**:1624–35.

36 Roberts AW, Seymour JF, Brown JR et al. Substantial susceptibility of chronic lymphocytic leukemia to BCL2 inhibition: results of a phase I study of navitoclax in patients with relapsed or refractory disease. J Clin Oncol 2012; **30**:488–96.

37 Shoemaker AR, Mitten MJ, Adickes J et al. Activity of the Bcl-2 family inhibitor ABT-263 in a panel of small cell lung cancer xenograft models. Clin Cancer Res 2008; **14**:3268–77.

38 Rudin CM, Hann CL, Garon EB et al. Phase II study of single-agent navitoclax (ABT-263) and biomarker correlates in patients with relapsed small cell lung cancer. Clin Cancer Res 2012; **18**:3163–9.

39 Mandik-Nayak L, Nayak S, Sokol C et al. The origin of antinuclear antibodies in bcl-2 transgenic mice. Int Immunol 2000; **12**:353–64.
40 Hughes P, Bouillet P, Strasser A. Role of Bim and other Bcl-2 family members in autoimmune and degenerative diseases. Curr Dir Autoimmun 2006; **9**:74–94.
41 Miret C, Font J, Molina R et al. Bcl-2 oncogene (B cell lymphoma/leukemia-2) levels correlate with systemic lupus erythematosus disease activity. Anticancer Res 1999; **19**:3073–6.
42 Cippa PE, Kraus AK, Edenhofer I et al. The BH3-mimetic ABT-737 inhibits allogeneic immune responses. Transpl Int 2011; **24**: 722–32.

Supporting information

Additional Supporting information may be found in the online version of this article at the publisher's Web site:

Fig. S1. Cell death upon ABT-737 is selective for peripheral blood (PBL). (a–c) C57-BL/6J-Fue and *Bim*$^{-/-}$ mice upon dextran sulphate sodium (DSS)-induced acute colitis (vehicle = white, ABT-737 = grey). Haematological analyses revealed (a) a significantly decreased number of lymphocytes and (b) a significantly increased number of granulocytes upon ABT-737 compared to vehicle controls. Analysis of variance (ANOVA) and Kruskal–Wallis ANOVA on ranks (Dunn's method). (c) ABT-737 levels were related directly to the removal of lymphocytes.

Fig. S2. Increased apoptosis in the spleen upon ABT-737 treatment. (a–d) C57BL/6 mice with dextran sulphate sodium (DSS)-induced acute colitis. (a) Haematoxylin and eosin (H&E) staining and terminal deoxynucleotidyl transferase dUTP nick end labelling (TUNEL)$^{+}$ cells (red) in spleen upon ABT-737 treatment. Mice treated with ABT-737 or vehicle received either (a) water or (b) DSS. Mice were killed at day 9. Treatment with ABT-737 was followed by an increase in TUNEL^{+} cells in both red pulp and white pulp. Images representative for five mice each. Original magnification as indicated. (c) Spleen weights in DSS-induced acute colitis in C57BL/6 mice. C57BL/6 mice were treated with ABT-737 or vehicle and received either water or DSS. Treatment with ABT-737 was followed by a decrease in spleen weight. Induction of colitis was followed by a significant increase of the spleen, shown to be decreased significantly upon ABT-737. Statistical analysis was performed using the Kruskal–Wallis one way analysis of variance (ANOVA), all pairwise multiple comparison procedures (Dunn's method), $P < 0{\cdot}05$ (*). (d) Spleen of a mouse which received vehicle (left) or ABT-737 (right) upon DSS. Images representative for 14 and 20 mice, respectively.

Fig. S3. Increased number of terminal deoxynucleotidyl transferase dUTP nick end labelling (TUNEL)$^{+}$ cells in Peyer's patches of the small bowel upon ABT-737 compared to vehicle treatment in the *IL-10*$^{-/-}$ model of spontaneous colitis. Mice upon ABT-737 or vehicle were killed at day 5. Original magnification × 630. Statistical analysis was performed using the Mann–Whitney rank-sum test, $P < 0{\cdot}05$ (*). The number of cells was calculated from four high-power fields for each mouse.

Fig. S4. Increased number of terminal deoxynucleotidyl transferase dUTP nick end labelling (TUNEL)$^{+}$ cells in Peyer's patches of the small bowel upon ABT-737. Water control mice upon vehicle or ABT-737. Mice were killed at day 9. Treatment with ABT-737 was followed by an increase in TUNEL^{+} cells in Peyer's patches of the small bowel. Images representative for five mice each. Original magnification as indicated.

Fig. S5. Increased number of terminal deoxynucleotidyl transferase dUTP nick end labelling (TUNEL)$^{+}$ cells in Peyer's patches of the small bowel upon ABT-737. Mice on dextran sulphate sodium (DSS) were killed at day 9. Treatment with ABT-737 was followed by an increase in TUNEL^{+} cells in Peyer's patches. Images representative for five mice each. Original magnification as indicated.

Fig. S6. Increased number of terminal deoxynucleotidyl transferase dUTP nick end labelling (TUNEL)$^{+}$ cells in Peyer's patches of the small bowel upon ABT-737 treatment in dextran sulphate sodium (DSS)-induced acute colitis in C57BL/6 mice. TUNEL^{+} cells frequently appeared as clusters of more than four cells in mice treated with ABT-737 compared to vehicle. Original magnification as indicated.

Fig. S7. Mice suffering from colitis develop an ameliorated intestinal inflammation upon ABT-737 treatment compared to vehicle-receiving mice. (a and b) C57BL/6 mice with dextran sulphate sodium (DSS)-induced acute colitis. (a) Representative images demonstrate colonoscopy pictures derived from ABT-737- and vehicle-treated mice. (b) Statistical analysis of colonoscopy score [murine endoscopic index of colitis severity (MEICS)]. Statistical analysis was performed using the Kruskal–Wallis one-way analysis of variance on ranks (Dunn's method).

Fig. S8. ABT-737 treatment was followed by a significant increase of the colon length. (a,b) Acute dextran sulphate sodium (DSS)-induced colitis in C57BL/6 mice. (a) Mice upon ABT-737 or vehicle received either water or DSS. Statistical analysis was performed using the one-way analysis of variance (ANOVA), all pairwise multiple comparison procedures (Bonferroni). (b) ABT-737 treatment was followed by a decrease in CD3^{+} in colonic lamina propria; original magnification × 10.

Fig. S9. ABT-737 treatment was followed by a significant increase of apoptosis in CD4^{+}CD62Lv in a dose-dependent manner. Contour plots. Following ABT-737 *in vivo* pretreatment CD4^{+}CD62L^{+} cells became susceptible to apoptosis initiated by ABT-737 compared to vehicle controls (ABT-737 concentration as indicated). Living cells, annexin V^{-}/propidium iodide (PI)$^{-}$; apoptotic cells, annexin V^{+}/PI^{-}.

Fig. S10. Depigmentation of the abdominal fur. Hair depigmentation after 56 days of long-term treatment of *IL-10*$^{-/-}$ with ABT-737 (50 mg/kg/3 days).